INTERNATIONAL SOCIETY FOR SOIL MECHANICS AND GEOTECHNICAL ENGINEERING

Examining the effects of layering on the seismic behavior of tailings dams using dynamic centrifuge tests

Zitao Zhang [i)], Jing Hu [ii)], Xuedong Zhang [i)], Leiji Qi [iii)] and Jianhui Liang [i)]

i) Senior Engineer, China Institute of Water Resources and Hydropower Research, Beijing, China.
ii) Engineer, China Institute of Water Resources and Hydropower Research, Beijing, China.
iii) M. Phil. Student, China Institute of Water Resources and Hydropower Research, Beijing, China.

ABSTRACT

This study aims to examine the effects of layering on the seismic behavior of tailings dams. The focus is put on the spatial distribution of excess pore pressure and its variations with time during earthquake loading. In order to achieve this, dynamic centrifuge tests have been carried out for tailings dam models with thin silty layers sandwiched in sandy tailings. The experimental results demonstrate that dense sandy tailings can be contractive under cyclic loading, generating excess pore pressure. The flow of liquid upwards to the slope surface and the dissipation of excess pore pressure in the tailings can be inhibited or slowed by the overlying silty layer. The tailings covered by silty layers at shallower locations may exhibit a more pronounced increase in the ratio of excess pore pressure over initial effective vertical stress, leading to a more significant reduction in the stiffness and strength. This eventually may lead to liquefaction or failure of the slope. Those results can improve our understanding on the seismic behavior of tailings pond with thin silty layers, which is common in real mining projects.

Keywords: dynamic centrifuge tests, tailings dam, liquefaction, layering, pore water pressure

1 INTRODUCTION

Enormous amount of wastes or tailings can be produced by the mining industry. For example, more than 5 t of tailings may be generated by the mining and milling processes in order to obtain about 10 g of gold (Aubertin et al., 1996). In order to restore those wastes, tailings dams which are among the largest and most critical geotechnical facilities have been widely constructed all over the world. In China, there are more than 13,000 tailings dams (Yu et al., 2014). Compared with the traditional water retention dams, tailings dams are more vulnerable to dam break or failure. As reported by Azam and Li (2010), the failure rate over the last one hundred years is about 1.2%, which is more than two orders of magnitude higher than the failure rate of water retention dams. As failure of tailings dams is usually followed by a fast-moving mudflow, catastrophic consequences can be caused (Santamarina 2019). For example, the mudflow triggered by the break of a tailings dam at Brumadinho, Brazil on 25 January 2019 killed about 235 people. Moreover, the failure of tailings dams and the associated massive mudflow have a huge impact on the local environmental and ecological systems. Therefore, it is essential to study the failure mechanisms of tailings dams.

Earthquake loading is one of the triggers of the failure of tailings dams (Dobry and Alvarez, 1967). For example, two tailings dams at Mochikoshi gold mine in Japan failed due to the Izu-Ohshima-Kinkai earthquake of 15 January 1978 (Ishihara, 1984). In order to shed light on the seismic response of tailings dams, dynamic centrifuge tests, which can simulate the real stress distribution and drainage condition in the field, have been carried out by different researchers. Zeng et al. (1998) carried out a series of tests on coal-waste tailings dams, and the experimental results provide clear evidence that the upstream tailings dam is more prone to fail than a similar structure built by the downstream method. Zhang et al. (2020) performed tests on clayey tailings reservoir founded on soft soil and suggest that the acceleration response increases with height for the tailings dam and the strongest acceleration response occurs at the highest sub-dam. Even though the excess pore pressure generated by earthquake loading is limited, severe lateral spreading can occur due to the little shear resistance of clayey tailings, which is also observed in Zeng et al. (1998). However, those tests were mainly on clayey tailings and a homogeneous soil profile was used. As indicated by Ishihara (1984), sandy tailings may sandwich thin layers with relatively low permeability in a real tailings pond. The effect of layering on the seismic response of tailings dams still remain not clear.

This study aims to characterize seismic behavior of sandy tailings dams with embedded relatively impermeable silty layers. In order to achieve this, dynamic centrifuge tests have been carried out in an advanced centrifuge shaking table. The focus is put on the spatial distribution of excess pore pressure and its variations with time.

2 EXPERIMENTAL DETAILS

2.1 IWHR horizontal-vertical centrifuge shaker

The IWHR horizontal-vertical centrifuge shaker is installed on a beam centrifuge, which has a capacity of 450 g-ton, a radius of 5.03 m, a maximum centrifugal acceleration of 300g and a maximum payload mass of 1.5 ton. As the world's first horizontal-vertical centrifuge shaker, the apparatus can simultaneously generate horizontal and vertical seismic motions at a centrifugal acceleration up to 100g, where g is the gravitational acceleration, enabling more accurate modeling of the in-situ seismic motion. The maximum model accelerations can reach up to 30g and 20g at horizontal and vertical directions, respectively. This ensures that a prototype earthquake wave with peak accelerations up to 0.75g and 0.5g at horizontal and vertical directions can be modeled at a centrifugal acceleration of 40g. The model frequency of input motions is in the range of 10 ~ 400 Hz. At a centrifugal acceleration of 40g, the frequency range is corresponding to 0.25 ~ 10Hz in the prototype scale, which covers the main frequency content of real earthquake waves.

Fig. 1. Photo of the IWHR horizontal-vertical centrifuge shaker

2.2 Model design

Fig. 2 gives a schematic drawing of the centrifuge model, which simulates a real upstream tailings dam. The centrifuge model was prepared in a flexible laminar container with inner dimensions of 800 × 360 × 620 mm in length, width, and height. The height of each laminar layer is about 21.5 mm. A 3 mm thick rubber bag is firstly placed in the inner space, and then the model of tailings dam was prepared in the rubber bag in order to avoid liquid leakage.

As shown in Fig. 2, the starter dam has a model height of 160 mm, and both the upstream and downstream slopes are 1:1.5. The same material is used in the tailings pond and sub-dams in this study, which has minor effect on the seismic response of the tailings dams. Hence, the tailings pond and the sub-dams are modeled by a slope of tailings. The model height of the tailings is 320 mm, and the downstream slope is 1:2.5. The tailings sandwich two 5 mm thick silty layers at model depths of 70 mm and 120 mm, respectively. Due to soil compression during spin-up of the centrifuge, the model settles and its

height is 304.8 mm before shaking at a centrifugal acceleration of 40g, hence, the corresponding prototype height is 12.2 m. There are in total 11 miniature pore pressure sensors from P1 to P11 in the tailings to monitor the pore pressure generation and dissipation. The location of each sensor has been marked in Fig. 2. In addition, the crest settlement is monitored by a laser displacement sensor.

The tailings material was collected from tailings pond of a gold mine in Gansu Province, China. This material can be categorized as silty sand, and the fractions of particles with sizes of 0.1 ~ 0.25 mm, 0.075 ~ 0.1 mm and < 0.075 mm are 28.8%, 40.0% and 31.2%, respectively. The maximum dry density is $1.592g/cm^3$, while the minimum one is $1.136 g/cm^3$. In this study, the dry density of tailings is $1.40 g/cm^3$ after sample preparation. Due to soil compression during spin-up of the centrifuge, the estimated dry density, void ratio and relative density are $1.47 g/cm^3$, 0.84, 79%, respectively. The relatively impermeable layer is prepared using kaolin, and the starter dam in prepared using coarse sand particles with sizes of 2 ~ 4 mm. Since the settlement of starter dam during spin-up is minor, its dry density at 40g is similar to the initial one, i.e., $1.62 g/cm^3$.

In reality, the tailings are nearly fully saturated, hence, the saturation condition should be fulfilled in the centrifuge tests. This may be achieved by adding liquid in the restored tailings, however, the liquid may drain quickly into the downstream part during spin-up of the centrifuge. In order to solve this problem, the centrifuge model is immersed in liquid to maintain the saturation condition during spin-up of the centrifuge and the subsequent shaking process. This has minor effect on the seismic response of the tailings dam. Moreover, in order to avoid the conflict of time scaling for consolidation and for the seismic motion, the viscosity of pore fluid is increased by 40 times by using a water solution of hydroxypropyl methylcellulose (HPMC).
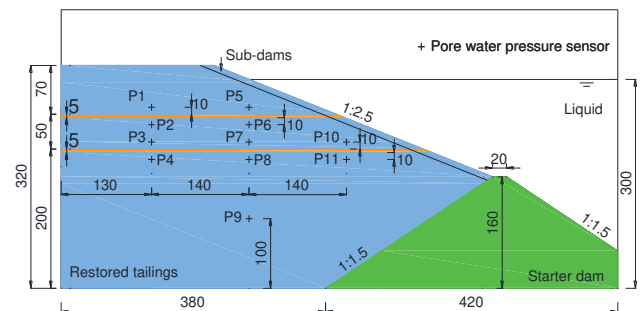

Fig. 2. Schematic drawing of the centrifuge model

After model preparation, the model was transferred to the centrifuge shaking table, followed by spin-up of the centrifuge. At a centrifugal acceleration of 40g, the model was subjected to horizontal bedrock motion perpendicular to the dam axis along the longitudinal direction of the container. Fig. 3 presents the recorded

bedrock acceleration using the accelerometer mounted on the shaking table. The prototype duration of the input motion is 400 s, which is much longer than the common durations of real earthquakes. However, since the peak bedrock acceleration is only 0.052g, the calculated Arias intensity which reflects input energy is only 0.8 m/s, which is in the range of typical values of real earthquakes.
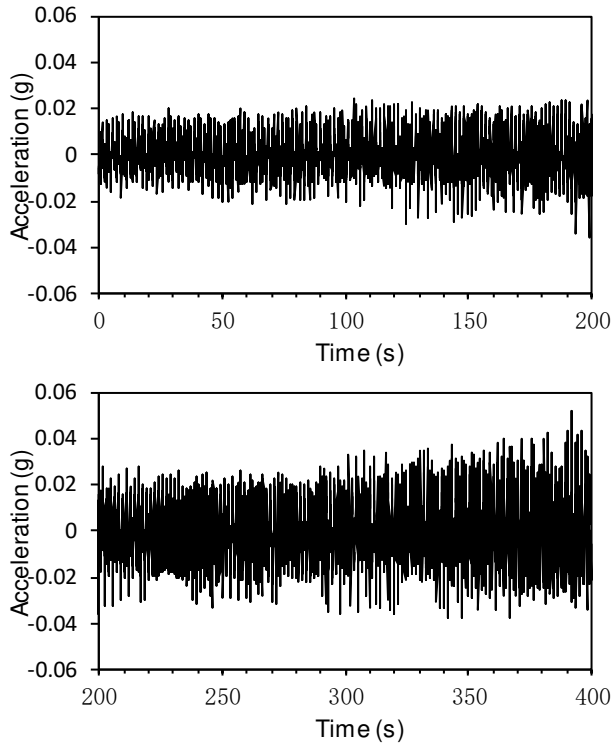

Fig. 3. Bedrock acceleration measured by the accelerometer mounted on the shaking table

3 EXPERIMENTAL RESULTS AND DISCUSSIONS

The experimental results are presented and discussed in the following. All the results are presented in prototype units unless indicated otherwise. No data associated with sensors P7 and P10 are herein shown as they did not work functionally during the experiment.

3.1 Crest settlement

The crest settlement induced by shaking is 60 mm at the end of shaking, which accounts for 0.5% of the initial dam height before shaking. This proves that the tailings dam did not fail, and only shallow sliding may occur during the process. The settlement is further compared with the values of concrete-faced rock-fill dams and earth-core dams (Zhang et al., 2019, Kim et al., 2011), which are smaller than 0.21% of the dam height. The settlement is relatively large in this study. This is reasonable as the martials used to build concrete-faced rock-fill dams and earth-core dams are much stronger than the tailings used in this study.

3.2 Horizontal distribution of excess pore pressure

Fig. 4 presents the variations in excess pore pressure in tailings with time, indicating that excess pore pressure has been generated at all locations. This reflects that dense sands can be contractive under cyclic earthquake loading, even though they are dilative under monotonic loading. This is similar to the observation in cyclic simple shear tests and cyclic undrained triaxial tests
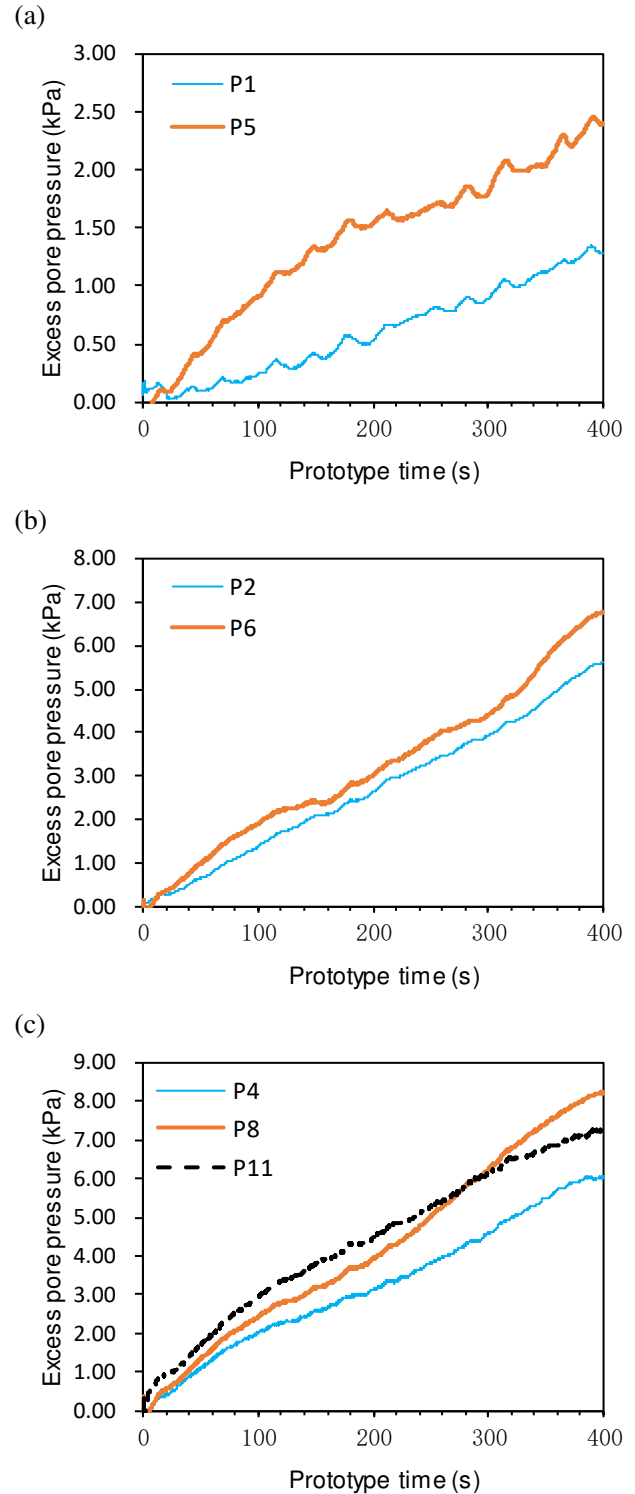

Fig. 4. Variations in excess pore pressure with time measured by sensors (a) P1 and P5, (b) P2 and P6 and (c) P4, P8 and P11.

(Ishihara and Takatsu, 1979; Yoshimi et al, 1989; Erten and Maher, 1995; Sze and Yang, 2013). In those tests, samples were subjected to a cyclic loading under a stress-controlled undrained condition after isotropic consolidation. The liquefaction state can be reached after a certain number of loading cycles, followed by severe double amplitude axial strain.

The excess pore pressures generated at the same depth are further compared in order to analyze the horizontal distribution of excess pore pressure. Fig. 4a compares the measurements at a shallower depth above the first silty layer. The excess pore pressure below sub-dams measured by P5 is larger than that measured by P1, which is in the tailings pond. Fig. 4b compares the measurements between the two silty layers. The relatively large value also occurs in the zone underneath sub-dams. Fig. 4c compares the measurements in tailings below the second layer. A similar trend is obtained, that is, the tailings underneath sub-dams (P8, P11) exhibit higher excess pore pressure.

The horizontal distribution of excess pore pressure affects the flow direction of liquid. To facilitate the discussion, the hydraulic gradients are further calculated. The hydraulic gradient from point A to B is denoted by i_{A-B}. For instance, i_{P5-P1} is the hydraulic gradient from P5 to P1. The magnitudes of i_{P5-P1}, i_{P6-P2} and i_{P8-P4} are 0.020, 0.021 and 0.036 at the end of seismic loading, respectively. The relatively low hydraulic gradient indicates the minor horizontal flow of liquid from the zone beneath the sub-dams to the pond. Assuming that the excess pore pressure at the downstream surface of sub-dams remain zero during shaking, the hydraulic gradient from P11 to the surface can be obtained. The value reaches 0.12 at the end of shaking, reflecting that considerable horizontal liquid flow can occur at the zone underneath the sub-dams during shaking.

3.3 Vertical distribution of excess pore pressure

Fig. 5 presents the distributions of excess pore pressure along vertical sections. Even though the data is limited, the trend suggests that the maximum excess pore pressure occurs in the zone near silty layer II. The areas in the upper and lower parts exhibit smaller excess pore pressures. Such spatial distribution of excess pore pressure implies that the pore liquid may flow upwards in the upper part and may flow downwards in the lower part.

Table 1 and Fig. 6 present the hydraulic gradients i_{P2-P1} and i_{P3-P2}. The gradient i_{P2-P1} keeps increasing with time during earthquake shaking, and the value reaches 0.46 at the end of shaking. The gradient i_{P2-P3} seems gradually saturated after an initial increment, and the final value reaches 0.14. The gradient i_{P2-P1} is more than three times larger than i_{P3-P2} after shaking. As i_{P2-P1} indicates the average gradient for the tailings and silty layer, the gradient in the silty layer is even larger than i_{P2-P1}. Due to the lack of measurements from P7, the gradient from P7 to P6 cannot be calculated. However,

as indicated in Table 1, the increasing trend of i_{P6-P5} is similar to that of i_{P2-P1}, and the final gradient reaches 0.47. This suggests that the gradient in silts is much larger than that in tailings.

Such kind of vertical distribution of hydraulic gradient provide possible explanations on the occurrence of sand volcanos which are often observed in the surface of disposal pond after earthquakes (e.g., Ishihara, 1984). Since the hydraulic gradient in silts keeps increasing with time or the energy of input motion, the hydraulic gradient in silts can be very high, hence, the highly compressed underlying tailings can be pumped out once the thin silty layer fails at some weak points, leading to the occurrence of sand volcanos.
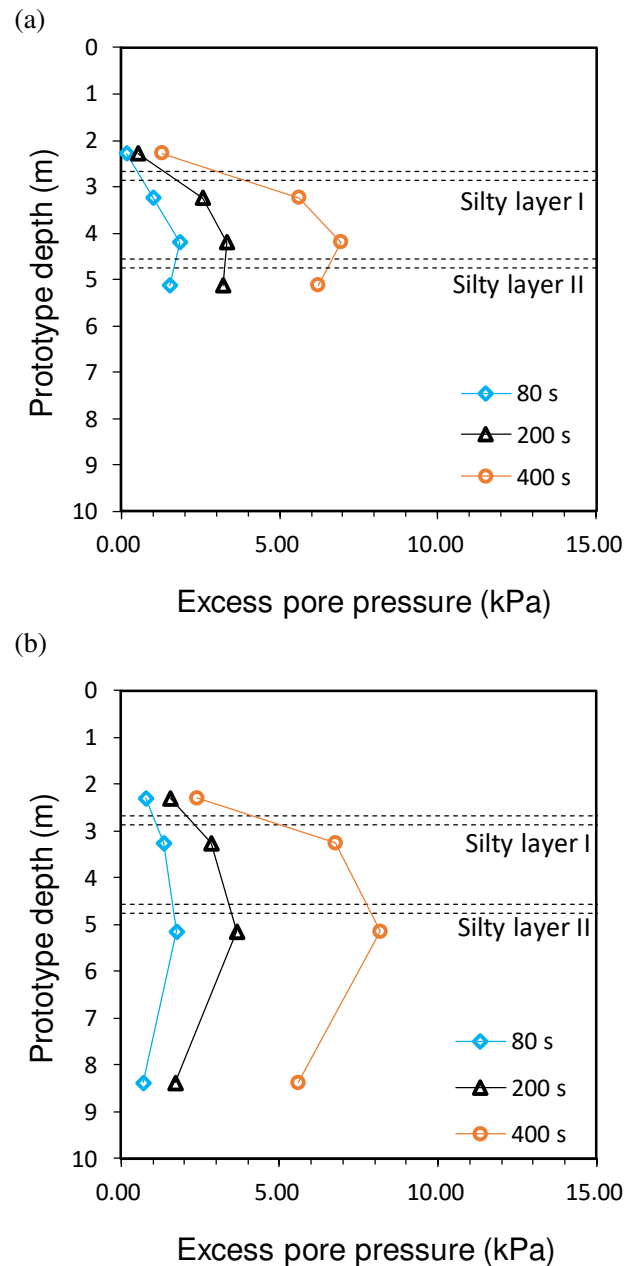
(a)

(b)

Fig. 5. Distributions of excess pore pressure (a) along a vertical section in the tailings pond and (b) along a vertical section below sub-dams
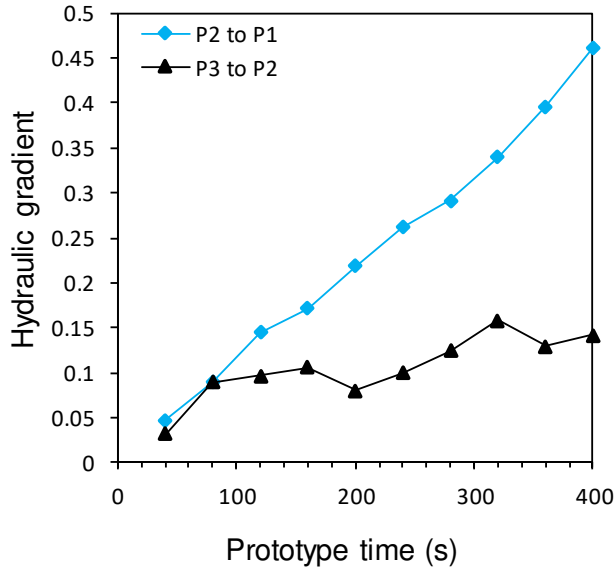
Fig. 6. Comparison of the hydraulic gradients i_{P2-P1} and i_{P3-P2}

Table 1. Summary of hydraulic gradients

Time (s)	40	80	120	160	200	240	280	320	360	400
i_{P2-P1}	0.05	0.09	0.14	0.17	0.22	0.26	0.29	0.34	0.40	0.46
i_{P3-P2}	0.03	0.09	0.10	0.11	0.08	0.10	0.12	0.16	0.13	0.14
i_{P6-P5}	0.04	0.06	0.12	0.09	0.14	0.21	0.21	0.28	0.38	0.47

3.4 Discussions on the effect of layering

The excess pore pressure can lead to lead to reduction in the effective stress of the soils, which may affect soil properties. The ratio (R_u) of excess pore pressure over initial effective vertical stress is generally used to describe the stress state of soils. To facilitate the discussion, the ratio at the end of shaking is calculated and summarized in Table 2. The maximum ratio R_u measured by the sensors is 35% at P11, and the spatial distribution of R_u can be used to examine the effect of layering.

For a homogeneous sandy ground, due to the increase of effective vertical stress with depth, the soils at shallower locations are more vulnerable to liquification than those at deeper locations, and the ratio R_u might keep decreasing with depth. Such a decreasing trend of R_u has been observed for the tailings between the two silty layers in this study. As shown in Table 2, the values at P2 is smaller than that at P3. This is also observed in the tailing near the second silty layer. The value beneath the second layer at P4 is smaller than that at P3. However, the tailings near the first silty layer demonstrates an opposite trend. The ratio R_u is 6% above the first silty layer at P1, while it increases to 19% at P2 underneath the first silty layer. The ratio R_u also increases from 11% at P5 to 23% at P6.

This demonstrates the effect of layering on the seismic behavior of tailings dams. The upward flow of liquid and the dissipation of excess pore pressure at shallower tailings can be inhibited or slowed by the overlying thin silty layer. The tailings covered by thin silty layers at shallower depths may exhibit a more pronounced increase in the ratio R_u, leading to a more significant reduction in the stiffness and strength of tailings. This eventually may cause liquefaction or failure of the slope. A similar mechanism is also used in explaining the slope failure at the Atlantic Frontier Environmental Network (AFEN) submarine slide complex (Madhusudhan et al, 2017).

Table 2. Ratio of excess pore pressure over initial effective vertical stress at the end of shaking

Sensor No.	P1	P2	P3	P4	P5	P6	P8	P9	P11
Ratio (%)	6	19	17	13	11	23	17	9	35

4 CONCLUSIONS

In this study, dynamic centrifuge tests have been performed to examine the effect of layering on the seismic behavior of tailings dams.

The experimental results demonstrate that dense sandy tailings can be contractive under cyclic loading, generating excess pore pressure. The flow of liquid upwards to the slope surface and the dissipation of excess pore pressure in the tailings can be inhibited or slowed by the overlying silty layer. The tailings covered by silty layers at shallower locations may exhibit a more pronounced increase in the ratio, leading to a more significant reduction in the stiffness and strength. This eventually may lead to liquefaction or failure of the slope.

The seismic response of tailings dams can be affected by many factors including the mechanical properties of materials, the geometrical characteristics of the slope, and characteristics of the input motion, e.g., frequency content and duration. Since only limited conditions were considered in this study, further experimental study is required to fully understand the effect of layering on the seismic response of tailings dams and to draw universal conclusions.

REFERENCES

1) Aubertin, M., Bussiere, B. and Chapuis, R. P. (1996): Hydraulic conductivity of homogenized tailings from hard rock mines, Canadian Geotechnical Journal, 33(3), 470-482.
2) Azam, S. and Li, Q. (2010): Tailings dam failures: a review of the last one hundred years, Geotechnical news, 28(4), 50-54.
3) Dobry, R. and Alvarez, L. (1967): Seismic failure of chilean tailing dams, Journal of the Soil Mechanics and Foundations Division, 93(6), 237-260.

4) Erten, D. and Maher, M. H. (1995): Cyclic undrained behavior of silty sand, *Soil Dynamics and Earthquake Engineering*, 14(2), 115-123.

5) Ishihara, K. (1984): Post-earthquake failure of a tailings dam due to liquefaction of the pond deposit, *Proceedings of First International Conference on Case Histories in Geotechnical Engineering*, 1129-1143.

6) Ishihara, K. and Takatsu, H. (1979): Effects of overconsolidation and K0 conditions on the liquefaction characteristics of sands, *Soils and Foundations*, 19(4), 59-68.

7) Kim, M. K., Lee, S. H., Choo, Y. W., et al. (2011): Seismic behaviors of earth-core and concrete-faced rock-fill dams by dynamic centrifuge tests, *Soil dynamics and earthquake engineering*, 31(11), 1579-1593.

8) Madhusudhan, B. N., Clare, M. A., Clayton, C. R. I. and Hunt, J. E. (2017): Geotechnical profiling of deep-ocean sediments at the AFEN submarine slide complex, *Quarterly Journal of Engineering Geology and Hydrogeology*, 50(2), 148-157.

9) Santamarina, J. C., Torres-Cruz, L. A. and Bachus, R. C. (2019): Why coal ash and tailings dam disasters occur, *Science*, 364(6440), 526-528.

10) Sze, H. Y. and Yang, J. (2014): Failure modes of sand in undrained cyclic loading: impact of sample preparation, *Journal of geotechnical and geoenvironmental engineering*, 140(1), 152-169.

11) Yoshimi, Y., Tokimatsu, K. and Hosaka, Y. (1989): Evaluation of liquefaction resistance of clean sands based on high-quality undisturbed samples. *Soils and Foundations*, 29(1), 93-104.

12) Yu, G. M., Song C. W., Pan Y. Z., et al. (2014): Review of new progress in tailing dam safety in foreign research and current state with development trent in China, *Chinese Journal of Rock Mechanics and Engineering*, 2014(S1), 3238-3248. (in Chinese)

13) Zeng, X., Wu, J. and Rohlf, R. (1998): Modeling the seismic response of coal-waste tailings dams, *Geotechnical News*, 6(6), 29-32.

14) Zhang, X. D., Cai, H., Wei, Y. Q., et al. (2020): Characterization of the seismic behavior of tailings reservoir founded on soft soil using dynamic centrifuge tests, *Rock and Soil Mechanics*, 41(4), 1-9. (in Chinese)

15) Zhang, X., Zhang, Z., Wei, Y., et al. (2019): Examining the seismic stress evolution in the face slab of concrete-faced rock-fill dams using dynamic centrifuge tests, *Soil Dynamics and Earthquake Engineering*, 123, 337-356.